Rear-Lamp Vehicle Detection and Tracking in Low-Exposure Color Video for Night Conditions

Ronan O'Malley, Edward Jones, *Member, IEEE*, and Martin Glavin, *Member, IEEE*

***Abstract*—Automated detection of vehicles in front is an integral component of many advanced driver-assistance systems (ADAS), such as collision mitigation, automatic cruise control (ACC), and automatic headlamp dimming. We present a novel image processing system to detect and track vehicle rear-lamp pairs in forward-facing color video. A standard low-cost camera with a complementary metal–oxide semiconductor (CMOS) sensor and Bayer red–green–blue (RGB) color filter is used and could be utilized for full-color image display or other color image processing applications. The appearance of rear lamps in video and imagery can dramatically change, depending on camera hardware; therefore, we suggest a camera-configuration process that optimizes the appearance of rear lamps for segmentation. Rear-facing lamps are segmented from low-exposure forward-facing color video using a red-color threshold. Unlike previous work in the area, which uses subjective color threshold boundaries, our color threshold is directly derived from automotive regulations and adapted for real-world conditions in the hue–saturation–value (HSV) color space. Lamps are paired using color cross-correlation symmetry analysis and tracked using Kalman filtering. A tracking-based detection stage is introduced to improve robustness and to deal with distortions caused by other light sources and perspective distortion, which are common in automotive environments. Results that demonstrate the system's high detection rates, operating distance, and robustness to different lighting conditions and road environments are presented.**

***Index Terms*—Computer vision, driver assistance, tail-lamp detection, vehicle detection, video processing.**

I. Introduction

RECENT statistics suggest that night conditions are an important area of focus for road safety. In the European Union, almost one third (32.7%) of road fatalities occur during hours of darkness [1]. Demand for advanced driver-assistance systems (ADAS) is expected to grow, as consumers grow increasingly safety conscious, and insurance companies and legislators begin to recognize the positive impact that such systems could have on accident rates. Automotive manufacturers have begun to introduce automatic cruise control (ACC) systems, which are mainly implemented with active sensors, such as radar. A forward-facing color camera could be a low-cost alternative or complementary technology to such active systems while also possibly fulfilling supplementary functions, such as lane-departure warning, pedestrian detection, or image display.

While driving at night, vehicles on the road in front are primarily visible by their red-color rear-facing tail and brake lamps. While all vehicles will differ in appearance, with different styles and designs of rear-facing lamps, they must adhere to automotive regulations. Worldwide regulations [2] (excluding regulations in the United States [3], which are less stringent) specify limits for color and brightness of rear vehicle lamps. While previous rear-lamp detection systems manually define subjective color and brightness thresholds, we utilize these regulations by deriving image processing system parameters from them. The regulations state that rear lamps must be placed symmetrically and in pairs; however, there is no specification restricting the shape of rear automotive lamps, and due to recent advances in light-emitting diode (LED) technology, lamp manufacturers are departing from conventional shapes of tail and brake lamps. Therefore, our detection method is cognizant of the regulations and is shape independent. As the appearance of rear lamps in video and imagery can dramatically change, depending on camera hardware, we suggest a camera-configuration process that optimizes the appearance of rear lamps for segmentation.

The target applications of this technology are ADASs, such as collision mitigation, ACC, and automatic headlamp dimming. While other elements may be required for a complete and comprehensive system (such as the classification of oncoming headlamps for automatic headlamp dimming systems), detection of rear lamps is a core component of each of the outlined potential target applications. The requirements of systems such as these are primarily the following: robust detection and tracking of vehicles in front, achievement of this within a reasonable distance, a low rate of false positive detections, and a measure of the distance between host and target vehicles. Systems should also be modular in nature and not tied to specific camera hardware. It is beneficial to use standard color cameras as they are of low cost, readily available, and practical, as the color video produced can be used for other ADAS utilizing color data and for full color display purposes. The layout of the remainder of this paper is given as follows: In Section II, we present a review of literature in the area of automotive vehicle detection, with particular emphasis on visual cameras and dark conditions. Section III outlines the camera-configuration process. The rear-lamp detection algorithm is described in Section IV. The tracking and tracking-based detection system elements are

Manuscript received July 23, 2009; revised November 6, 2009 and March 1, 2010; accepted March 2, 2010. Date of publication April 12, 2010; date of current version May 25, 2010. This work was supported by the Irish Research Council for Science, Engineering and Technology Embark Initiative. The Associate Editor for this paper was M. Á. Sotelo Vázquez.

The authors are with the Connaught Automotive Research Group, Electrical and Electronic Engineering, National University of Ireland, Galway City, Ireland (e-mail: ronan.omalley@nuigalway.ie; edward.jones@nuigalway.ie; martin.glavin@nuigalway.ie).

This paper has supplementary material provided by the authors. This includes five multimedia AVI format movie clips, which display sample results of the proposed tail lamp detection algorithm. This material is 3.2MB in size.

Color versions of one or more of the figures in this paper are available online at http://ieeexplore.ieee.org.

Digital Object Identifier 10.1109/TITS.2010.2045375

described in Section V. Experimental results are presented in Section VI. We conclude and consider possibilities for future work in Section VII.

II. State of the Art

The techniques commonly employed for vehicle detection under daylight conditions have comprehensively been reviewed in [4]. Most of the features employed for daylight vehicle detection have limited use under dark conditions and at night. Vehicle shadows, horizontal and vertical edges, and corners are difficult or impossible to detect in darkness, and the most significant preceding vehicle features in dark environments are rear-facing lamps.

Vehicular rear lamps appear as some of the brightest regions in a frame of night-time automotive video; therefore, it is common for image processing techniques for lamp detection to begin with some form of thresholding. Grayscale or brightness thresholding is a common starting point [5]–[8]. The resultant pixels are then grouped and labeled to analyze characteristics, such as area, position, and shape. Further filtering is required as there are many potential light sources that are not rear vehicle lamps, such as street lamps, headlamps of oncoming vehicles, and reflections from signs.

Employing a red-color filter has been shown to be an effective way to remove nonvehicle light sources. Many different color spaces with widely varying parameters have been used to segment red-color light regions from images; however, all have been based on subjective color boundaries. No known previous research detects automotive rear lamps based on the red-color limits set out by regulations. The most common approach makes use of the red–green–blue (RGB) color space [9]–[13]. Separate RGB thresholds for brightness and redness are implemented in [12], whereas in [9], only the red channel of the RGB data is analyzed. However, bright nonred lights can have a significant red-color component; therefore, analysis of the red channel alone is not sufficient for red-color thresholding. The RGB color space has also been used for detection of red vehicle lamps under daylight conditions [14].

The RGB color space is not ideal for the task of color thresholding; it is difficult to set and manipulate color parameters due to high correlation between the R, G, and B channels [15]. Other research in the area has opted to use other color spaces for a red-color threshold to overcome this difficulty. Cabani *et al.* use the L^*a^*b color space to segment red vehicle lamps [16], because it requires only two-color threshold operations, compared with three for RGB, and is hence more computationally efficient. However, this advantage is somewhat negated as the data must first undergo a color space transformation. The red-color threshold parameters were also subjectively chosen. Grayscale algorithms can also be applied using only the lightness channel L. The YCbCr space is used to detect the redness of lamps in [17], where the red-difference chroma channel Cr is analyzed to distinguish which bright areas are red light sources.

The appearance of rear lamps in captured video and imagery is highly dependent on the camera settings and sensor characteristics and varies widely among previous work. It has been observed that tail lamps usually appear as white regions with red surroundings as they can partially saturate image sensors [9], [11]. The perimeter of the saturated white regions is analyzed in [11], and if the surrounding area is comprised mostly of red pixels, it is regarded as a potential rear lamp.

The task of detecting tail lamps can considerably be aided by utilizing novel and nonstandard camera hardware. Current commercial systems use custom novel hardware filters. Non-Bayer patterns with combinations of red and clear filters have proven to be effective in detecting red lamps and differentiating between tail lamps and other light sources [18], [19]. Another commercial system uses two coated lenses (with one blocking red light and one allowing only red light to pass) to focus incoming light onto different parts of a single imaging sensor [20], [21]. While custom hardware can have performance advantages, these cameras cannot produce color images; therefore, they cannot be reused for other ADASs that use color image processing and have limited use in terms of displaying video to the driver. Custom hardware also adds cost and complexity to automotive systems.

Physical assumptions have been used to filter potential light candidates and aid the detection process. It has been assumed that rear lamps are circular or elliptical in shape [5], [13], [22]. However, the shape of rear lamps is not specified in the regulations, and as LED automotive lamps become more prevalent, rear lamps are being manufactured in radically different shapes. The average target vehicle is assumed to be approximately 170 cm wide in [13], and the width/height aspect ratio of a highway vehicle is assumed to be approximately 2.0. In [11], the assumption that most rear lamps are 70–90 cm above the ground is made. Lane detection is commonly employed to focus attention and prioritize an area of the frame [11], [13], [23].

Once tail-lamp candidates have been detected in an image, a system must be put in place to pair them to associate the detected lamps with a target vehicle. A close vertical position [13] and a similar area [11] of lamp regions have been used as the pairing criteria. In [10], the aspect-ratio constraints of resulting bounding boxes are considered since it can be assumed that the resulting box will generally be relatively flat and wide. In [5], comparisons between the horizontal and vertical coordinates of candidates are examined, coupled with a search for a license plate between them. Alcantarilla *et al.* detected headlights reliably up to 50 m in grayscale video [8] utilizing a support vector machine classifier.

Symmetry is commonly used to filter potential candidates [24] and create lamp pairs for vehicle detection, because the rear of a vehicle is symmetrical under all lighting conditions. In [25], symmetry is calculated within a candidate bounding box and considered with several other features in a weighted fusion process. In [9], the symmetry axis is the vertical axis of the tracking window.

At night time, symmetry is a useful tool for classifying and pairing rear lamps as regulations state that they must be symmetrical and placed in pairs. In [23], correlation between potential headlamp pairs is calculated to assess symmetry. Lights belonging to the same vehicle have high correlation values as they will have very similar size, shape, and luminance values. Correlation is frequently used in computer vision for

matching detections against a template or searching an image for a template. The assumption that the target vehicle will appear symmetrical is based on the assumption that it is pointing in approximately the same direction as the host vehicle so that foreshortening is negligible [12]. However, this assumption is not valid when there are perspective distortions, e.g., in situations such as overtaking maneuvers, lane changes, or sharp bends. Symmetry of rear-lamp pairs can be affected when other vehicle lamps are engaged, such as turn signal lamps, or when other light sources appear close to the rear lamps, such as oncoming headlamps. No known prior work addresses the issue of these frequently occurring distortions.

Temporal continuity of video data can be used to improve detection rates and the robustness of vehicle detection systems. Kalman filtering is a well-known approach for target tracking, which uses a Gaussian distribution density to represent the target. It estimates the state of a dynamic system from a series of incomplete or noisy measurements and can continue tracking through short occlusions [26]. It uses the previously estimated state and the current measurement (if available) to estimate the current state of the system. The Kalman filter has been used for multivehicle tracking [27]. A vehicle lamp's trajectory has been used to distinguish it from static lights, such as street lamps and reflective road signs [28]. In [29], a mean-shift estimator is used for tracking vehicles during daytime. Bayesian templates, in conjunction with a Kalman filter, are used in [30] for tracking of vehicles during daylight conditions. A particle filter is used in [25] to merge multiple target cues, including tail lamps.

III. Camera Configuration

Differences between acquisition systems can have a substantial effect on the properties of the captured images. The color and intensity of pixels from rear lamps will vary, depending on the properties of the camera that captures the image and its configuration. This problem has not directly been addressed in any known prior work, meaning that results cannot accurately be replicated or verified, and a technique cannot easily be transferred to different camera hardware. We propose a two-stage camera configuration: First, we set a static exposure level based on an ANSI photography standard so that the light levels do not saturate the camera sensor, ensuring that maximum color information is available in the captured image frame. Second, we consider color consistency so that the device-dependent digital color data can be compared with the device-independent visible light color boundaries defined in automotive regulations. These configurations also ensure that images of rear lamps are not affected by ambient lighting conditions.

A. Exposure Control

Control of camera exposure is essential to the process of photographing light sources. With too low an exposure, the target can appear too dark, such that the image detail can be lost. With too high an exposure, the intensity of the light can cause saturation in the image, where color and shape information can be lost. By default, most cameras typically implement an automatic exposure control algorithm. However, these algorithms are generally optimized for daylight operation and are not suited for detecting color light sources at night. In images captured with automatic exposure, rear lamps typically appear oversaturated. This "blooming" effect, where lamps appear as large saturated regions [see Fig. 1(a)], has been noted by others and has even been used for detection [11]. However, this saturation is generally considered to be undesirable as all color information is lost in saturated pixels and the appearance of vehicle lamps significantly changes between different lighting conditions, as the exposure is adjusted to compensate for overall scene light level changes, such as going between lit and unlit environments.

(a) (b)

Fig. 1. Example of (a) video frame captured with the automatic exposure control enabled and (b) video frame captured using a lower static exposure [$\mathrm{EV}_{100} = 10$]. Note how the rear lights in (a) saturate, resulting in the lights appearing white, whereas, in (b), the color of the red lights is preserved. However, in (b), much of the lower intensity background detail from the scene is not present, due to the lower exposure.

High dynamic range (HDR) cameras have been used to detect traffic signals at night [31]. HDR cameras intelligently fuse high- and low-exposure images, which results in an image that captures detail of high- and low-intensity regions. Since we are only interested in the high-intensity parts of the image for this application, we can replicate some of this HDR functionality by setting a low exposure with regular camera hardware to ensure that the color detail of high-intensity light sources is captured. The result of this is that lower intensity detail, which is not of interest to this system, is lost in the resultant scene. This reduction in low-intensity detail further simplifies the lamp segmentation process; an example of the image from this configuration is shown in Fig. 1(b).

Previous work in traffic-signal detection at night has utilized a low static exposure value (EV) [32]; however, most research in automotive lamp detection does not address the issue of exposure control. Camera exposure is determined by three parameters: 1) exposure time (*shutter speed*); 2) aperture (*F-number*); and 3) sensitivity (*ISO value*). An EV [33] can be calculated from these variables. This value can be transferred between cameras to ensure equivalent levels of exposure between different hardware. EV is defined by

$$\mathrm{EV}_{ISO} = \log_2 \frac{N^2}{t} \tag{1}$$

where N is the aperture stop, t is the exposure time, and ISO is the camera sensitivity. The ANSI photography standard exposure guide [34] recommends an EV_{100} of 9–10 for neon lights and other bright signs. We propose adopting this value for exposure control, setting a static EV of 10 for the task of detecting automotive rear lamps. This is comparable to the manually calibrated static EV of 12.3 set in [32] for traffic signal detection.

The regulations specify that the minimum acceptable intensity of tail lamps is 4 cd, whereas the maximum acceptable intensity of brake lamps is 185 cd. To investigate the suitability of our chosen static exposure setting, we considered images of two extreme situations: 1) brake lamps at the shortest operating distance and 2) tail lamps at the maximum operating distance. With this exposure configuration, at 3 m, brake lamps will partially saturate in the image, with typically 10%–15% of the pixels saturating. Although saturation is not desirable, an amount of it is tolerated by the lamp segmentation algorithm outlined in Section IV. If exposure were to be lowered until there was no saturation in the lamp image at close range, the maximum operating distance of the system would be reduced. The maximum operating distance was determined by analyzing tail-lamp images at various known distances. Experiments have shown that the maximum distance that tail lamps can reliably be detected with our configuration is 50 m, with initial detection between 50 and 80 m. At greater distances, tail lamps appear to be too dim or are too small in area to be reliably detected. Therefore, this exposure setting offers a satisfactory tradeoff between the close-distance saturation level and the maximum operating distance.

Ambient lighting conditions are usually a significant factor in photography when configuring a camera. The color and intensity of ambient light are usually important factors to consider, and video cameras typically implement automatic exposure and white balance algorithms by default to compensate for changes in ambient lighting. Objects in the scene being captured are visible, because they reflect some of this ambient light. However, when photographing a light source such as a tail lamp, the lamp is visible because of the light emitted from its light source. The intensity of ambient light reflected from the surface of the lamp is negligible by comparison. Therefore, with a static exposure configuration, changes in ambient lighting conditions, such as driving from a lit to an unlit area of road, do not have a significant effect on the appearance of the lamps.

B. Color Configuration

The camera is configured to disable all automatic color-processing operations, including automatic white balance, as this artificially distorts color information. The gray-world assumption used in most automatic white balance algorithms is not a valid assumption at night. We set a manual white balance to the reference white point of the color gamut of the camera. Our camera hardware uses PAL color specification, for which the white point is the CIE Standard Illuminant D65 (6500 K). This configuration ensures that ambient scene illumination is not a significant factor in color representation. The influence of reflected light from external light sources on the captured pixel color of the tail and brake lamps is negligible.

IV. Red Light Detection

In this section, we describe the structure of our image processing algorithm that extracts and pairs rear vehicle lamps from frames of forward-facing automotive video. Bright objects such as street lamps, traffic signals, turn signal lamps, oncoming headlamps, and reflections from road infrastructure are filtered out while retaining the rear lamps of target vehicles as regions of interest (ROIs). Segmented red lamps are then paired to associate them with a target vehicle.

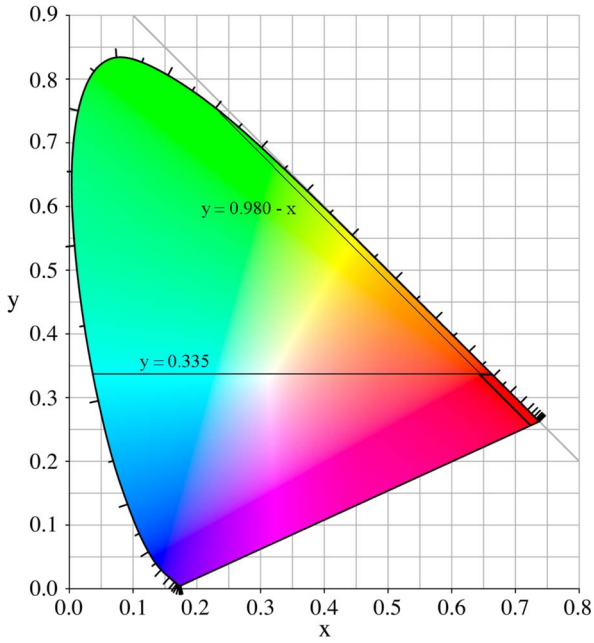

Fig. 2. CIE 1931 xy chromaticity diagram showing the regulation limits of light for red rear automotive lamps.

A. Deriving HSV Color Threshold

The trichromatic coordinates specifying the regulation color for red rear lamps [2] are defined by the following inequalities:

$$\text{Limit toward yellow}: \quad y \leq 0.335 \tag{2}$$

$$\text{Limit toward purple}: \quad y \geq 0.980 - x. \tag{3}$$

These inequalities can be observed on the CIE xy chromaticity diagram in Fig. 2, with the area of acceptable visible light encompassed by the two linear limits. To derive color threshold parameters from these limits, we transform the enclosed region into the PAL RGB color space (the gamut of our camera hardware). The thresholds specified in the regulations and the chromaticity diagram are in 2-D xy space. However, this is a 2-D representation of the 3-D xyY color space, and the luminance dimension Y is omitted from the diagram. For conversion to RGB, we transform all luminance values. The transform of this 3-D CIE xyY region to PAL RGB is conducted through the CIE XYZ color space [35]. The first step is to convert the xyY region to XYZ using the following:

$$X = \frac{xY}{y} \tag{4}$$

$$Z = \frac{(1-x-y)Y}{y} \tag{5}$$

$$Y_{(XYZ)} = Y_{(xyY)}. \tag{6}$$

The luminance dimensions in these spaces are the same; hence, they have the same symbol. This XYZ space is then converted to PAL RGB (7)–(9)

$$[r \quad g \quad b] = [X \quad Y \quad Z][M]^{-1} \tag{7}$$

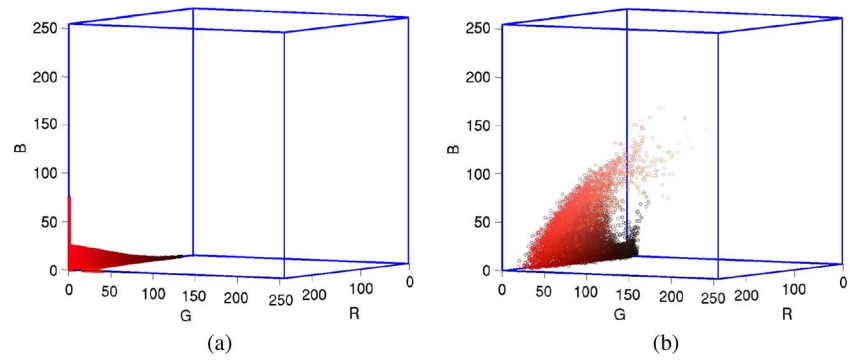

Fig. 3. (a) Rear-lamp regulation red-color region transformed into RGB space. (b) RGB scatter plot of pixels from a database of tail and brake lamp images.

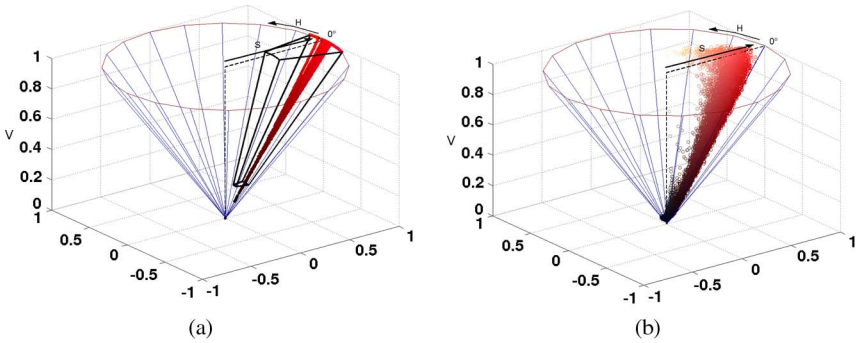

Fig. 4. Rear-lamp regulation red-color region mapped to conical HSV color space. (a) Highlighted section represents the derived color threshold value limits. (b) Conical HSV scatter plot of pixels from a database of tail and brake lamp images.

where $[M]^{-1}$ is the inverse transformation matrix. This can be calculated from the reference primary coordinates of the color system, which, for PAL RGB, results in

$$[M]^{-1} = \begin{pmatrix} 3.240454 & -0.969265 & 0.055643 \\ -1.537138 & 1.875010 & -0.204025 \\ -0.498531 & 0.041555 & 1.057225 \end{pmatrix}. \quad (8)$$

The final RGB values are calculated using the gamma value of the color space γ, which, for PAL RGB, is 2.2

$$R = r^{\frac{1}{\gamma}}, \qquad G = g^{\frac{1}{\gamma}}, \qquad B = b^{\frac{1}{\gamma}}. \quad (9)$$

The resulting regulation color region in RGB space is shown in Fig. 3(a). Observe the "tail" segments splitting from the main region. These artifacts are the result of clipping at the maximum R level. This is because the regulation color region specified extends outside the color gamut of the most common RGB spaces used in digital imaging, such as sRGB, PAL, and NTSC.

A database of 300 tail and brake lamp images was created to observe the color distributions of rear-lamp pixels. Fig. 3(b) shows an RGB distribution of pixels from this database. It can be observed from this scatter plot that red rear-lamp pixels do not directly conform to the derived regulation region. To adapt the regulation color region to real-world images, we convert it into the hue–saturation–value (HSV) color space as it is more intuitive to adjust and manipulate the threshold parameters than RGB. HSV is best represented as an inverted cone, with hue (tint) as the angle (0°–360°), saturation (shade) as the radius (0–1), and value (tone) as the perpendicular height (0–1). The color red is located around the hue value of 0°. We convert the regulation color region from RGB to the HSV space [36]. This is shown in Fig. 4(a).

TABLE I
HSV COLOR THRESHOLD VALUES

	Minimum	Maximum
Hue (H)	342°	9°
Saturation (S)	0.4645	1.0
Value (V)	0.2	1.0

The H threshold limits were directly extracted from the limits of this distribution. The V component of the distribution spans the entire range of possible values. However, it is undesirable to allow the entire range of V values through the color threshold, as hue and saturation are inaccurate and unpredictable at very low levels of V, and many background pixels would be allowed through. We therefore block the lowest V values from the threshold. Fig. 4(b) shows an HSV scatter plot of pixels taken from the database of tail and brake lamp images.

While the regulations specify fully saturated color for rear lamps, the saturation component of a color is somewhat dependent on the intensity of the incident light. It can be observed from Fig. 4(b) that pixels from the database of lamp images occupy a range of saturation values. We derive the S threshold limit from a histogram of these saturation levels. A Gaussian curve was fit to the histogram data, and the threshold was established at 0.4645, which is the lower 95.4% normal probability point $(\mu - 2\sigma)$. These final threshold values are presented in Table I and overlaid on Fig. 4(a).

The input frame is median filtered to reduce noise before performing a color threshold with these values. This produces

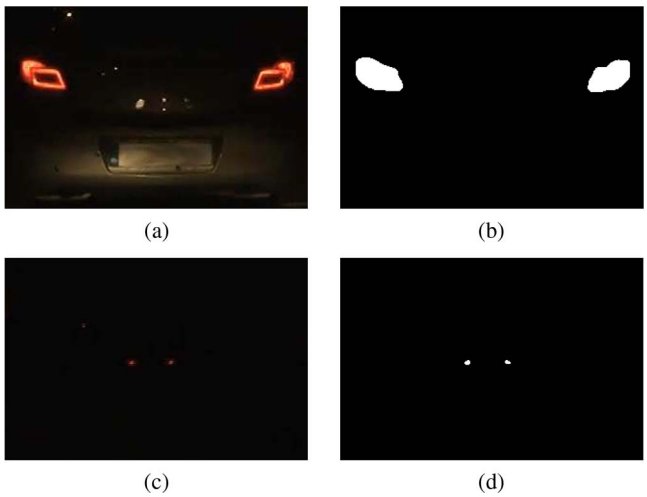

Fig. 5. (a) and (c) Low-exposure forward-facing night video frames and (b) and (d) their resulting binary images from the HSV color threshold and morphological closing. Tail and brake lamps are successfully extracted, whereas other light sources are excluded.

a binary image indicating the position of red lamp pixels in the image. This is morphologically closed to remove noise and merge together closely located lamp segments, which may have been segmented by the color threshold. Examples of the result of this color thresholding are presented in Fig. 5. Red tail and brake lamp light sources are successfully extracted, whereas other common light sources, such as street lamps and signs, are excluded.

B. Light Candidate Pairing

Although the shape of automotive rear lamps is not specified by regulations, rear-lamp pairs must be symmetrical. Image cross correlation has previously been used in automotive vision systems for headlamp detection [23] and template matching of vehicles [9]. We use fast normalized cross correlation [37] to measure the symmetry between rear-lamp candidates. Correlation is calculated along the direction of a line adjoining the center of each light, as in [23]. This compensates for differences in roll angle between host and target vehicles caused by subtle variations in road surface and camera placement. One of the lamp regions is horizontally mirrored and used as the template T; this is then compared against the image of the potential matching lamp I. The cross-correlation matrix γ is calculated between two lamp image segments by

$$\gamma = \sum_{x,y} \frac{\left(T(x,y) - \bar{T}\right)\left(I(x,y) - \bar{I}\right)}{\sigma_T \sigma_I} \tag{10}$$

where $\bar{T}$ and $\bar{I}$ are the mean values of T and I, respectively, and σ_T and σ_I are the standard deviations of T and I, respectively. To utilize color information, correlation matrices are calculated for R, G, and B channels, and the mean is calculated. A lamp pair is classified as a valid vehicle if the maximum value in the cross-correlation matrix γ is greater than a threshold $\gamma_{\min}$. The value for this was derived from the distribution of the correlation coefficients for a database of 300 images containing valid vehicle lamp pairs, as shown in Fig. 6. A Gaussian curve

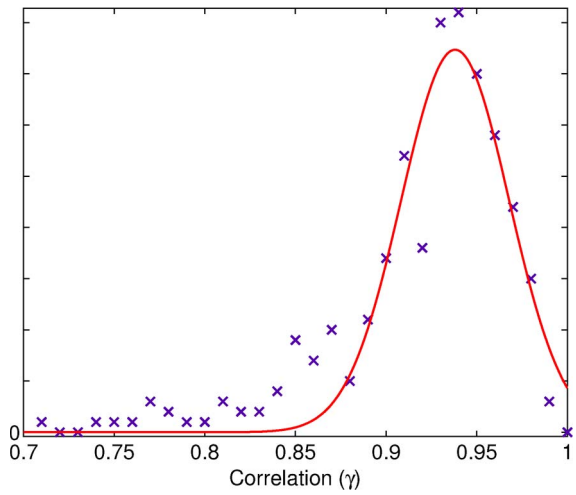

Fig. 6. Histogram illustrating the distribution of cross-correlation values γ from a database of vehicle images and a Gaussian curve fit to the data ($\mu = 0.9381, \sigma = 0.0421, \mu - 2\sigma = 0.8538$, and RMSE $= 2.192$).

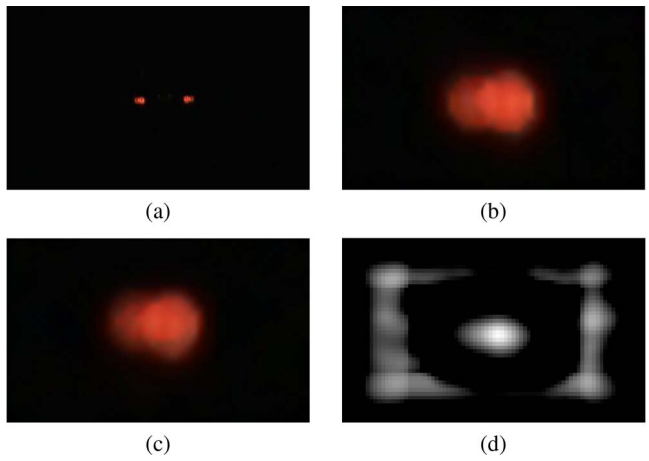

Fig. 7. Result of rear-lamp cross-correlation pairing process. (a) Original low-exposure forward-facing image. A vehicle is clearly visible by its tail lamps. (b) Median filtered image of the left tail lamp. (c) Median filtered and horizontally mirrored image of the right lamp. (d) Result of the normalized cross correlation γ. The maximum value is located at the center and is 0.97, indicating a 97% correlation and a valid vehicle lamp pair.

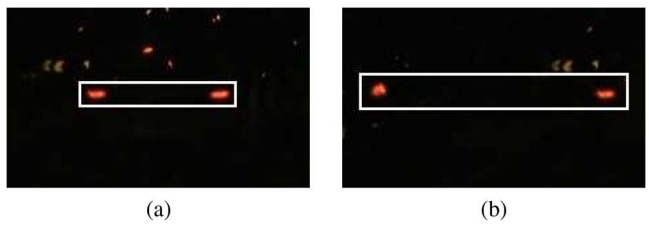

Fig. 8. (a) Valid vehicle tail lamp pair and correlation $\gamma = 0.8874$. (b) Similarly sized lamps from different vehicles and correlation $\gamma = 0.5771$.

was fit to the histogram data, and the threshold was established at the lower 95.4% probability point $(\mu - 2\sigma)$. This results in a pairing correlation threshold of $\gamma_{\min} = 0.8538$. This approach is a size- and shape-independent method of pairing detected lamps. Fig. 7 shows example lamp images and the resulting cross-correlation matrix. Examples of a valid lamp pair, a pair of similarly sized nonidentical lamps, and their respective correlation values are shown in Fig. 8.

There are many benefits to using cross correlation to pair light candidates. This method is not directly dependent on the result of the threshold stage. The binary result of the threshold is used only to generate ROIs in the source image for correlation. Some pairing algorithms apply heuristics to the properties of the binary thresholded regions such as comparison of vertical position or centroid, region size or area, and bounding box aspect ratio. These methods are dependent on, and sensitive to, the result of the threshold. Further issues with these methods are that they do not consider color or intensity information and that they may not produce a numerical parameter that is representative of how well two regions are matched. If they do, and several properties are analyzed, a method must be formed to weigh or average the parameters. Our cross correlation utilizes the color data from the source image and produces a single numerical parameter, indicating how well the regions are matched. These methods can also be sensitive to the size and shape of target regions. More advanced methods attempt to fit an axis of symmetry to candidate pairs. This can be quite processing intensive and is more appropriate for symmetry analysis in more complex situations, such as vehicle detection in daylight conditions.

V. Tracking and Tracking-Based Detection

A. Kalman Filter Tracking

We perform tracking to smooth detection noise and vehicle movement noise, to interpolate position during short periods where detection has failed, and to predict the future position of targets, thus aiding temporal association between frames. For tracking, we use the Kalman filter [38], [39], a least-squares estimation of linear movement with an efficient implementation, as it only requires the tracking estimate from one previous frame to be stored in memory.

Once classified as vehicles, we track targets using the four parameters of a bounding box surrounding the lamp pair (x-position, y-position, width, and height); these form a state vector $\hat{x}$. First, predictions of the state vector $\hat{x}^-$ and state error covariance matrix P^- are generated for a target at time k, i.e.,

$$\hat{x}_k^- = A\hat{x}_{k-1} \tag{11}$$

$$P_k^- = AP_{k-1}A^T + Q \tag{12}$$

where A is the state transition matrix, and Q is the process noise covariance matrix. These predictions are then used to associate detections in the current frame with targets being tracked. These system measurements z are used to correct and update the corresponding trackers. The Kalman gain K is computed by

$$K_k = P_k^- H^T \left(HP_k^- H^T + R\right)^{-1} \tag{13}$$

where H is the matrix that relates the true state space with the measurement space, and R is the measurement noise covariance matrix. This Kalman gain is then used to correct the previous estimate of state and error covariance, i.e.,

$$\hat{x}_k = \hat{x}_k^- + K_k\left(z_k - H\hat{x}_k^-\right) \tag{14}$$

$$P_k = (I - K_k H)P_k^-. \tag{15}$$

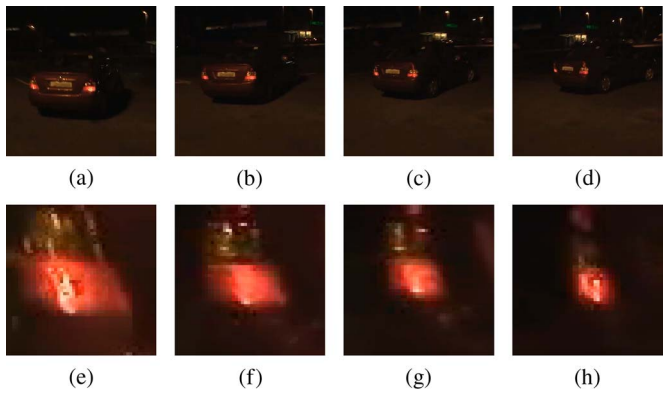

Fig. 9. (a)–(d) Frames from a video of a close-range vehicle progressing through 45° right turn. (e)–(h) Enlarged view of the perspective distortion undergone by the left tail lamp during the maneuver.

The measurement covariance parameter R determines the sensitivity of the tracker to updates. Higher values of measurement covariance will mean less weighing on the current measurements and smoother movement, whereas lower values will mean heavier weighing on the current measurements and a more responsive tracker. However, if this parameter is too low, the tracker can become unstable during occlusions and detection failures, and therefore, there is a tradeoff when choosing a value for R. For our video data (720×576 pixels and 25-Hz frame rate), an R value of 0.1 was found to be suitable for ensuring that the vehicle tracker was responsive yet remained stable during noise caused by variations in road terrain.

B. Tracking-Based Detection

It was observed from preliminary testing that extended detection failure was commonly a result of the distortion of the symmetry between target rear lamps. Rear-facing lamps can become distorted by external light sources, such as oncoming headlamps or turn signal lamps. Because of our low-exposure configuration, there is significantly less blooming than systems that utilize automatic exposure control. However, distortion in the appearance of lamps remains an issue. The symmetry of a target may also be disrupted due to perspective distortion, where there is a difference in yaw angle between the host and target vehicles.

These distortions can cause symmetry checks to fail, because the lamps may no longer appear to be symmetrical, i.e., they are no longer the same size, shape, or color. We address this problem by examining predicted tracker areas when they fail to update with a new detection. The cross correlation between pixels in the current predicted target location and lamp regions from the previous detection is calculated. If there is a correlation greater than 70% for at least one of the lamps, the tracker is updated with the new location. This adds extra robustness to the system for situations where symmetry is distorted, but at least one of the lamps maintains its appearance.

This technique also ensures that the tracking mechanism continues to update during perspective distortions when the appearance of both lamps slowly changes. An example case of perspective distortion of a turning vehicle is shown in Fig. 9. The enlarged view of the left tail lamp shows that it reduces in

TABLE II
SUMMARY OF EXPERIMENTAL RESULTS—BY ENVIRONMENT TYPE

Environment	Pre-Tracking Detection Rate (%)	Post-Tracking Detection Rate (%)	False Positive Rate (%)
Urban	93.2880	97.4177	4.6315
Rural	93.1769	96.8653	1.3112
Motorway	92.4720	97.5105	1.8207
Mean	92.9790	97.2645	2.5878

size and horizontally condenses as the vehicle turns. As this gradually happens (with respect to the video frame rate), an average correlation of 82% is maintained between lamp images between frames, and the vehicle is tracked throughout the turn.

VI. RESULTS

Experimental data were captured using a forward-facing camera mounted inside the host vehicle, behind the rear view mirror. The color video was captured using a regular camera with a CMOS sensor and a Bayer RGB filter. It should be noted that a Bayer RGB sensor effectively has one third the spatial resolution of a grayscale sensor, such as that used in [8], and two thirds of the spatial resolution of the clear/red sensor used in [18]. The video was processed at a resolution of 720 × 576 pixels at 25 Hz. More than 5 h of on-road video were captured, comprising speeds ranging from 0 to 100 km/h. We present video results categorized into three environment sets: 1) urban; 2) rural; and 3) motorway, with each set containing 30 video segments of 20 s in duration. In total, 45 000 test images containing vehicles, which were taken from 5 h of on-road video, were processed, and the results were manually classified. Video segments categorized as urban were captured in lit, inner city, and suburban environments. Video segments in the rural category were captured on unlit country roads, whereas motorway environment video segments were recorded on lit and unlit multilane dual carriageways and motorways.

Table II presents the detection rates before and after tracking and the false positive rates for each environment type. We define detection rate as the number of frames with successful detection and pairing of valid vehicle lamp pairs out of the total number of frames. The detection rate after tracking is the number of frames where the tracker successfully updates with new detection measurements or tracking-based detection measurements out of the total number of frames. Finally, the false positive rate is the total number of false detections in proportion to the total number of frames. Fig. 10 contains several result frames from the experimental data set.

We can deduce from these results that detection results do not widely vary between environments. Slightly higher post tracking detection rates in urban and motorway environments may be attributed to the generally consistent road surface, which reduces camera shake, simplifying the tracking process. The highest false positive rate was from video data recorded in an urban environment. False positives were most commonly caused by background light sources, such as street lamps and other road vehicle lamps. The majority of false positive detections appear for only single frames and are easily filtered. The rural environment presented the fewest number of false positives, which can be attributed to the relatively few background light sources, compared with the other environments.

Fig. 10. Successful vehicle detection result frames and enlarged view (inset), representative of results from the experimental data set. These vehicles are detected at distances of (a) 4 m, (b) 15 m, (c) 59 m, and (d) 72 m.

Fig. 11. Results of successful tracking-based detection (a) when one of the tail lamps is distorted because of a turn signal lamp or (b) when both are distorted due to perspective distortion when the target vehicle is turning at an angle.

The tracking algorithm increases the detection rate for two reasons: First, failed detections are frequently only for a small number of frames. In these situations, the tracking algorithm prediction is used until the target is redetected. Second, tracking-based detection has demonstrated robustness to distortions caused by background light sources, as well as perspective distortion caused by the target vehicle's relative position or yaw angle. Fig. 11 shows examples of successful tracking-based detection in both of these scenarios.

Our assumption that the target vehicle is symmetrical generally holds when it is in the same lane as the host vehicle or at distances greater than 15 m if in a neighboring lane on a straight section of the road. Situations where this assumption does not hold are during sharp bends, turns, interchanges, and the latter stages of overtaking maneuvers. When the vehicle is already detected and being tracked before such a maneuver occurs, our tracking-based detection algorithm maintains detection of the vehicle while both lamps are still visible. When overtaking a target vehicle on a straight road, it was found that our algorithm successfully detected and tracked the target vehicle until it exited the frame at approximately 10 m, and target vehicles

TABLE III
SUMMARY OF EXPERIMENTAL RESULTS—BY DISTANCE

Distance Range	Detection Rate (%)
0-15m	96.5827
15-30m	98.5067
30-50m	94.9645

TABLE IV
DETECTION PERFORMANCE COMPARISON OF DIFFERENT CAMERAS

Camera	10m	20m	30m	40m	50m	60m	70m	80m
1	•	•	•	•	•	•	•	
2	•	•	•	•	•	•		
3	•	•	•	•	•	•		

were continuously tracked through tight bends as both lights, although distorted, remain visible.

As the appearance of a target vehicle is highly dependent on its distance from the camera, the distance is obviously an important factor to consider in analyzing the performance of the system. Distance to target vehicles was estimated from video using the perspective projection equation for a pin-hole camera model that was used and described in [9] and [8]. Table III presents the system detection rate after tracking, which was classified by distance. Our system has a high detection rate for vehicles up to 50 m away, whereas vehicles are commonly initially detected between 50 and 80 m. These results are comparable with the state-of-the-art grayscale results [8].

Failure to detect target vehicles was most commonly caused by lack of intensity or insufficient resolution of vehicles that were greater than 50 m away. At these distances, rear lamps can appear faint and are sometimes not sufficiently intense to satisfy the color threshold. At the resolution of our data, a vehicle tail lamp at 80 m may be less than ten pixels in size. Potential ways to improve on this could be to implement a dynamic exposure control system to ensure the optimal intensity of target tail lamps or to process video data captured at a higher resolution. As megapixel image sensors become more common in vehicles and automotive embedded hardware advances, in vehicles, high-definition video processing will become feasible.

To evaluate the sensor independence of the system, test images were captured at a range of distances using three different cameras. Each camera was configured according to Section III, and images were all scaled to the same resolution. While it is not appropriate to directly compare color threshold results from different cameras, we can compare them in terms of detection results for the same test scenarios. Test images of the rear of a stationary vehicle were taken with each camera at 10-m intervals of distances from up to, and including, 80 m. The results of these tests are presented in Table IV. The vehicle was successfully detected at each distance by each camera image up to 50 m, demonstrating comparable performance between different cameras. There were slight differences in results between cameras at 70 m at the limits of when the vehicle is first detected.

Transitions from tail lamp to brake lamp and vice versa are flawlessly handled, and neither detection nor tracking is interrupted. Numerous target vehicles in the test video were modern and had LED tail lamps. Their high-frequency pulsed luminance did not cause problems; they appear with consistent intensity in each frame and are detected with the same accuracy as regular bulb lamps.

These results confirm that our system satisfies each of the requirements of the target automotive safety applications as set out in Section I. Robust detection of targets is achieved, with a low occurrence of false positives. An approximation of the distance to the detected vehicles is calculated, and the maximum detection distance of the system is comparable with the state of the art. The system is modular in design and is not tied to specific camera hardware.

VII. CONCLUSION

In this paper, we have described a system that detects vehicles in front at night using a regular-color forward-facing camera. We have described the advantages of using standard-color camera hardware, as opposed to a novel or specialized platform. We have presented a camera configuration process that addresses the issues of reproducing and verifying results, portability between different camera hardware, and ensuring lamp color information is not lost due to pixel saturation. Red-color thresholds have been derived from automotive regulations and adapted to real-world conditions utilizing the HSV color space, as opposed to subjective color thresholds or hardware color filters used in related research. We have presented a shape- and size-independent color image cross-correlation approach to pairing detected lamps. A Kalman-filter-tracking algorithm has been implemented to improve robustness by ensuring continuity of operation through small detection failures and predicting future location of targets. A tracking-based detection algorithm has been implemented to make the system robust to distortions of symmetry. Results from on-road testing have been presented, demonstrating the system's high detection rate and robustness in different environments.

Future work may include the development of an embedded implementation of this system incorporating an automatic exposure control algorithm that dynamically ensures optimum appearance of target lamps. This may extend the operating range of the system, as well as demonstrate real-time system performance. High-definition video data may also be investigated as a means to further increase the operating range.

REFERENCES

[1] "Traffic Safety Basic Facts 2007—Motorways," Eur. Road Safety Observatory, 2007.
[2] "Regulation no. 7, Uniform Provisions Concerning the Approval of Front and Rear Position (Side) Lamps, Stop-Lamps and End-Outline Marker Lamps for Motor Vehicles (Except Motor Cycles) and Their Trailers," UN World Forum Harmonization Vehicle Regulations, 1968.
[3] "Federal Motor Vehicle Safety Std. 108," Nat. Highway Trafic Safety Admin., Tech. Rep.
[4] Z. Sun, G. Bebis, and R. Miller, "On-road vehicle detection: A review," *IEEE Trans. Pattern Anal Mach. Intell.*, vol. 28, no. 5, pp. 694–711, May 2006.
[5] N. Alt, C. Claus, and W. Stechele, "Hardware/software architecture of an algorithm for vision-based real-time vehicle detection in dark environments," in *Proc. Conf. Design, Autom. Test Eur.*, 2008, pp. 176–181.
[6] S.-C. Kim and T.-S. Choi, "Fast vision-based vehicle detection algorithm using recognition of light pattern," in *Proc. Appl. Digital Image Process. XXIII*, 2000, vol. 4115, pp. 654–661.

[7] S.-Y. Kim, S.-Y. Oh, J.-K. Kang, Y.-W. Ryu, K.-S. Kim, S.-C. Park, and K.-H. Park, "Front and rear vehicle detection and tracking in the day and night times using vision and sonar sensor fusion," in *Proc. IEEE/RSJ Int. Conf. Intell. Robots Syst.*, Aug. 2005, pp. 2173–2178.
[8] P. Alcantarilla, L. Bergasa, P. Jimenez, M. Sotelo, I. Parra, D. Fernandez, and S. Mayoral, "Night time vehicle detection for driving assistance lightbeam controller," in *Proc. IEEE Intell. Vehicles Symp.*, Jun. 2008, pp. 291–296.
[9] M. Betke, E. Haritaoglu, and L. S. Davis, "Real-time multiple vehicle detection and tracking from a moving vehicle," *Mach. Vis. Appl.*, vol. 12, no. 2, pp. 69–83, Aug. 2000.
[10] Y.-L. Chen, "Nighttime vehicle light detection on a moving vehicle using image segmentation and analysis techniques," *WSEAS Trans. Comput.*, vol. 8, no. 3, pp. 506–515, Mar. 2009.
[11] M.-Y. Chern and P.-C. Hou, "The lane recognition and vehicle detection at night for a camera-assisted car on highway," in *Proc. IEEE Int. Conf. Robot. Autom.*, Sep. 2003, vol. 2, pp. 2110–2115.
[12] R. Sukthankar, "Raccoon: A real-time autonomous car chaser operating optimally at night," in *Proc. IEEE Intell. Vehicles Symp.*, Jul. 1993, pp. 37–42.
[13] C.-C. Wang, S.-S. Huang, and L.-C. Fu, "Driver assistance system for lane detection and vehicle recognition with night vision," in *Proc. IEEE/RSJ Int. Conf. Intell. Robots Syst.*, Aug. 2005, pp. 3530–3535.
[14] L. Gao, C. Li, T. Fang, and Z. Xiong, *Vehicle Detection Based on Color and Edge Information*. Berlin, Germany: Springer-Verlag, 2008, ser. Lecture Notes in Computer Science, pp. 142–150.
[15] H. Cheng, X. Jiang, Y. Sun, and J. Wang, "Color image segmentation: Advances and prospects," *Pattern Recognit.*, vol. 34, no. 12, pp. 2259–2281, Dec. 2001.
[16] I. Cabani, G. Toulminet, and A. Bensrhair, "Color-based detection of vehicle lights," in *Proc. IEEE Intell. Vehicles Symp.*, Jun. 2005, pp. 278–283.
[17] S. Nagumo, H. Hasegawa, and N. Okamoto, "Extraction of forward vehicles by front-mounted camera using brightness information," in *Proc. IEEE Can. Conf. Elect. Comput. Eng.*, May 2003, vol. 2, pp. 1243–1246.
[18] G. P. Stein, O. Hadassi, N. B. Haim, and U. Wolfovitz, "Headlight, taillight and streetlight detection," U.S. Patent 7 566 851 B2, Jul. 28, 2009.
[19] A. López, J. Hilgenstock, A. Busse, R. Baldrich, F. Lumbreras, and J. Serrat, *Nighttime Vehicle Detection for Intelligent Headlight Control*. Berlin, Germany: Springer-Verlag, 2008, ser. Lecture Notes in Computer Science, pp. 113–124.
[20] C. Schadel and D. Falb, "Smartbeam—A high-beam assist," in *Proc. Int. Symp. Automotive Lighting*, Darmstadt, Germany, 2007.
[21] J. H. Beschtel, J. S. Stam, and J. K. Roberts, "Vehicle vision based systems having improved light source distinguishing features," U.S. Patent 7 408 136 B2, Aug. 5, 2008.
[22] R. Taktak, M. Dufaut, and R. Husson, "Vehicle detection at night using image processing and pattern recognition," in *Proc. IEEE Int. Conf. Image Process.*, 1994, vol. 2, pp. 296–300.
[23] R. Cucchiara and M. Piccardi, "Vehicle detection under day and night illumination," in *Proc. Int. ICSC Symp. Intell. Ind. Autom.*, 1999, pp. 789–794.
[24] W. Liu, X. Wen, B. Duan, H. Yuan, and N. Wang, "Rear vehicle detection and tracking for lane change assist," in *Proc. IEEE Intell. Vehicles Symp.*, Jun. 2007, pp. 252–257.
[25] Y.-M. Chan, S.-S. Huang, L.-C. Fu, and P.-Y. Hsiao, "Vehicle detection under various lighting conditions by incorporating particle filter," in *Proc. IEEE Intell. Transp. Syst. Conf.*, Sep. 2007, pp. 534–539.
[26] E. Cuevas, D. Zaldivar, and R. Rojas, "Kalman filter for vision tracking," Freie Universität Berlin, Inst. Informatik, Berlin, Germany, Tech. Rep. B 05-12, 2005.
[27] D. Koller, J. Weber, and J. Malik, *Robust Multiple Car Tracking With Occlusion Reasoning*. Berlin, Germany: Springer-Verlag, 2006, ser. Lecture Notes in Computer Science, pp. 189–196.
[28] C. Julià, A. Sappa, F. Lumbreras, J. Serrat, and A. López, "Motion segmentation through factorization. Application to night driving assistance," in *Proc. Int. Conf. Comput. Vis. Theory Appl.*, 2006, pp. 270–277.
[29] K. She, G. Bebis, H. Gu, and R. Miller, "Vehicle tracking using on-line fusion of color and shape features," in *Proc. IEEE Int. Conf. Intell. Transp. Syst.*, Oct. 2004, pp. 731–736.
[30] F. Dellaert and C. Thorpe, "Robust car tracking using Kalman filtering and Bayesian templates," in *Proc. SPIE Conf. Intell. Transp. Syst.*, 1998, vol. 3207, pp. 72–83.
[31] F. Lindner, U. Kressel, and S. Kaelberer, "Robust recognition of traffic signals," in *Proc. IEEE Intell. Vehicles Symp.*, Jun. 2004, pp. 49–53.
[32] F. Kimura, T. Takahashi, Y. Mekada, I. Ide, and H. Murase, "Recognition of traffic signals in various conditions for safety driving assistance," in *Proc. MIRU*, 2006, pp. 618–623 (in Japanese).
[33] S. Ray, *Manual of Photography: Photographic and Digital Imaging*, 9th ed. Oxford, U.K.: Focal, 2000, ch. Camera Exposure Determination, pp. 310–335.
[34] American National Standard for Photography, "Photographic exposure guide," Amer. Nat. Stand. Inst., Tech. Rep. ANSI PH2.7-1986, 1986.
[35] B. Lindbloom. (2010, Mar.). [Online]. Available: http://www.brucelindbloom.com/
[36] A. Smith, "Color gamut transform pairs," *ACM SIGGRAPH Comput. Graph.*, vol. 12, no. 3, pp. 12–19, Aug. 1978.
[37] J. P. Lewis, *Fast Normalized Cross-Correlation*. San Rafael, CA: Industrial Light and Magic, 1995.
[38] R. E. Kalman, "A new approach to linear filtering and prediction problems," *Trans. ASME, J. Basic Eng.*, vol. 82, pp. 35–45, Mar. 1960.
[39] G. Welch and G. Bishop, "An introduction to the Kalman filter," Dept. Comput. Sci., Univ. North Carolina, Chapel Hill, NC, Tech. Rep. TR 95-041, 2003.

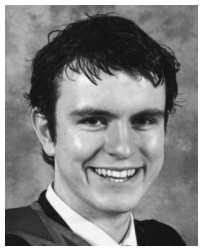

Ronan O'Malley received the B.E. degree in electronic and computer engineering in 2006 from the National University of Ireland, Galway (NUIG), Ireland, where he is currently working toward the Ph.D. degree in automotive image processing, with particular focus on vulnerable road-user detection at night.

He joined the Connaught Automotive Research Group, Electrical and Electronic Engineering, NUIG, in 2006. His research interests include automotive technology, vision systems, and image processing.

Edward Jones (M'91) received the B.E. and Ph.D. degrees in electronic engineering from the National University of Ireland, Galway (NUIG), Ireland.

He is currently a Lecturer with Electrical and Electronic Engineering, NUIG. He has previously been with Toucan Technology Ltd. and PMC-Sierra Inc., developing digital signal processing (DSP) algorithms for digital-subscriber-line modems. From 2001 to 2002, he was a Senior DSP Architect with Innovada Ltd., developing software for embedded voice-band modem technology, and from 2002 to 2003, he was with Duolog Technologies Ltd., where he developed DSP algorithms and implementations for wireless networking systems (including wireless local area networks). His current research interests are DSP algorithm development for applications in image processing, speech processing, and biomedical engineering.

Martin Glavin (M'95) received the Diploma degree in electronic engineering in 1994 and the Honors degree in electronic engineering and the Ph.D. degree in advanced equalization techniques for high-speed digital communications from the National University of Ireland, Galway (NUIG), Ireland, in 1997 and 2004, respectively.

Since 1999, he has been a Lecturer with Electrical and Electronic Engineering, NUIG. His research interests are image processing and embedded systems in the areas of automotive systems and biomedical signal processing.